Investigation of oxidation state-dependent conformational changes in *Desulfovibrio vulgaris* Hildenborough cytochrome c_{553} by two-dimensional ^{1}H-NMR spectra

Laurence Blanchard[a], Martin J. Blackledge[b], Dominique Marion[b,*], Françoise Guerlesquin[a,**]

[a]*Laboratoire de Bioénergétique et Ingénierie des Protéines, CNRS, 13402 Marseille Cedex 20, France*
[b]*Laboratoire de Résonance Magnétique Nucléaire, Institut de Biologie Structurale Jean-Pierre Ebel, CNRS-CEA, 38027 Grenoble Cedex 1, France*

Received 11 April 1996

Abstract Two-dimensional nuclear magnetic resonance spectroscopy (2D-NMR) was used to assign the proton resonances of ferricytochrome c_{553} from *Desulfovibrio vulgaris* Hildenborough. The spin systems of 76 out of 79 amino acids were identified by *J*-correlation spectroscopy (COSY and HOHAHA) in H_2O and D_2O and correlated by nuclear Overhauser effect spectroscopy (NOESY). The proton chemical shifts are compared in both oxidized and reduced states of the protein at 23°C and pH 5.9. Chemical shift variations between reduced and oxidized states are due to the paramagnetic contribution. Medium and long-range nOe demonstrate the lack of major changes between the two redox states. NMR data provide evidence that in this low oxidoreduction potential cytochrome, the oxidized state is more rigid than the reduced state.

Key words: Ferricytochrome c_{553}; *Desulfovibrio*; Two-dimensional NMR; Paramagnetic shift; Low oxidoreduction potential

1. Introduction

Cytochromes *c* are implicated in a wide variety of biological electron-transport processes, such as aerobic and anaerobic respiration and photosynthesis. The oxidoreduction potential of these proteins is apparently related to the metabolism of the organism and varies over a range from +640 mV for *Thiobacillus ferrooxidans* cytochrome c_{552} to −400 mV for *Desulfovibrio* cytochrome c_3. To date, the structural basis for the control of the oxidoreduction potential in cytochromes has remained unclear.

The amino-acid sequence comparison of 96 mitochondrial cytochromes *c* and 20 cytochromes c_2 reveals that 26 of the 104 amino acids of horse cytochrome *c* are constant [1]. The key roles of conserved residues (in protein folding and structure, oxidoreduction potential modulation or electron-transfer kinetics) can be established by site-directed mutagenesis. Recently, single-site mutants of these conserved residues have been reported for four eukaryotic and one prokaryotic species (yeast iso-1 and iso-2 cytochromes, *Drosophila melanogaster* cytochrome *c* [2], rat cytochrome *c* [3] and *Rhodobacter capsulatus* cytochrome c_2 [4]). Minor changes in the oxidoreduction potential (< 50 mV) [5] have been reported, except when the iron ligands are directly modified [6]. The 1000 mV oxidoreduction potential differences probably originate from more global structural variations. Structural characterization of low oxidoreduction potential cytochromes has shed light on the structure/oxidoreduction potential relationships in *c*-type cytochromes. The structures of two low potential cytochromes have been reported: *Chlorobium thiosulfatophilum* cytochrome c_{555} (+145 mV) by radiocrystallography [7] and NMR [8] and *Ectothiorhodospira halophila* cytochrome c_{551} (+58 mV) by NMR [9]. Lower oxidoreduction potentials are found in cytochromes *c* from sulfate-reducing bacteria which are strict anaerobic organisms. *Desulfovibrio* cytochrome c_{553} (M_r 9000) exhibits the same heme binding site (Cys-2aa-Cys-His) and sixth ligand as bacterial and mitochondrial cytochromes *c* but possesses little sequence homology with them.

Previous 1D-NMR studies of *D. vulgaris* Hildenborough and *D. desulfuricans* Norway cytochromes c_{553} have described some structural characteristics of these proteins, in particular the methionine heme axial ligand geometry of coordination [10]. A change in the conformation was suggested between the two oxidoreduction states, which would involve an inversion of the chirality of the methionine (at the S-CH_3 level), a finding not previously observed. Nakagawa et al. [11] gave preliminary crystallographic results on the oxidized state of *D. vulgaris* Miyazaki cytochrome c_{553} which presents 80% identity with Hildenborough strain cytochrome c_{553}. The NMR-based 3D structure of ferrocytochrome c_{553} from *D. vulgaris* Hildenborough has been recently obtained [12,13] and compared to a representative structure from the bacterial and mitochondrial cytochrome *c* family [14,15]. Although the secondary structures of the two proteins seem highly conserved, it is quite hazardous to speculate on the location of the possible structural changes induced by the oxidoreduction transitions, as the α-carbon structure reported by Nakagawa et al. [11] exhibits too low a resolution for reliable comparison. We have thus undertaken a 2D-NMR study of the ferricytochrome c_{553}. Here, we report the ^{1}H resonance assignment of the ferricytochrome and analyze the secondary structure of the protein on the basis of nOe. The structural parameters obtained from 2D-NMR on both states are compared and considered on the basis of the structural changes found in mitochondrial cytochrome *c* oxidation/reduction transition [16].

*Corresponding author. Fax: (33) 76-88-54-94.

**Corresponding author. Fax: (33) 91-16-45-78.

Abbreviations: 1D/2D, one/two-dimensional; TOCSY, total correlation spectroscopy; COSY, correlation spectroscopy; DQF-COSY, double quantum filtered correlation spectroscopy; NOESY, nuclear Overhauser effect spectroscopy

This is publication No. 265 of the Institut de Biologie Structurale Jean-Pierre Ebel.

PII S0014-5793(96)00580-7

2. Materials and methods

2.1. Sample preparation

D. vulgaris Hildenborough cytochrome c_{553} was expressed in *D. desulfuricans* G200. The purification of recombinant cytochrome has already been reported [17]. NMR samples were prepared in potassium phosphate buffer (0.1 M, pH 5.9). Two samples were used, one in 90% H_2O and 10% D_2O and one in D_2O, at a protein concentration of 8 mM. The D_2O sample was obtained after successive lyophilization and incubation for 1 h at 35°C.

2.2. ^{1}H-NMR spectroscopy

All the NMR experiments were recorded on a Bruker AMX 600, processed at ^{1}H=600 MHz. For nOe measurements involving heme methyl protons or methyl protons of the axial methionine, the one-dimensional truncated driven method [18] was preferred, because of the short relaxation time of these protons (mixing times in the range 150–250 ms were used) [19,20]. 2D spectra were collected at 14, 23 and 37°C. Chemical shifts were calibrated with respect to H_2O, and calibrated in turn at 4.658 ppm at 37°C, 4.792 ppm at 23°C and 4.878 ppm at 14°C with 2,2-dimethyl-2-silanepentane-5-sulfonate (DSS). Two-dimensional (2D) spectra were processed using either the UXNMR software of the Bruker spectrometer or Felix software provided by Hare Research, Inc. (Bothell, WA). All 2D spectra were recorded in the phase-sensitive mode using the hypercomplex method [21]. *J*-correlated spectra were obtained by either double-quantum-filtered COSY [22] or TOCSY [23] experiments and nOe-correlated spectra by NOESY [24] experiments. For NOESY and TOCSY spectra in H_2O buffer, the water resonance was eliminated by a combination of weak presaturation ($\gamma B_2 \approx 50$ Hz) and jump-and-return [25] just prior to the detection period. As nOe cross-peaks with paramagnetically shifted resonances are preferably detected by 1D-NMR, the 2D-NMR spectra were extensively folded in both dimensions ($SW(F_2)$=15.1 ppm and $SW(F_1)$=12.0 ppm). The choice of unequal spectral widths makes it possible to easily discriminate wrap-around resonances from true signals.

3. Results

3.1. Sequential assignment

As compared to previous spectra recorded on the ferrocytochrome c_{553}, all NMR data exhibit a substantial line broadening. This relaxation effect has a direct effect on the signal-to-noise in any 2D experiment but it is particularly salient in the case of 2D correlation spectra involving transverse coherence transfer such as COSY and TOCSY. In the COSY experiments, several NH/CαH correlations were missing, as a result of the cancellation of broad antiphase components. Similarly, the transfer by isotropic mixing from the NH to the protons of long side chains is not complete, which makes the assignment of these residues more laborious. As the line broadening was surprisingly amplified at 37°C as compared to 23°C, the assignment was carried out at lower temperature.

Because of better spectral quality, the assignment was initiated on D_2O spectra, where few slowly exchanging protons are still observable. The two stretches detected in D_2O (37–44 and 69–79) correspond to helical structures. These fragments extend further beyond the limits found under similar conditions for the ferrocytochrome (38–42 and 69–77) [12] and this result indicates an increased stability of the oxidized state.

The second step of the assignment was the identification of the four helices previously described in the ferrocytochrome c_{553} structure, using the NH to NH cross-peaks in H_2O NOESY spectra (see Fig. 1) and then the loops between the helices. Combination of TOCSY and NOESY spectra at 14, 23 and 37°C was necessary to corroborate the full assignment presented in Table 1. For comparison of the two redox states, the ferrocytochrome spectra were reassigned at 23°C.

The two N-terminal residues as well as G12 were not identified (as for the reduced cytochrome). Among the 25 long spin systems, the 12 lysines were assigned up to the εCH_2, the proline and arginine were fully assigned. Q32 was particularly well resolved, the 5 glutamic acids were not significantly affected by the paramagnetic effect, and only two of the five methionines (M56 and the 6th heme ligand, M57) were notably shifted.

The chemical shifts of the tyrosine rings are drastically affected by the concurrent effect of the pseudo-contact shift and flipping rate variation possibly due to a more rigid structure. Y38, Y49 and Y64 ring protons, which are rapidly flipping in the reduced protein, give rise to two broader signals at 23°C. In the reduced protein, both Y7 and Y75 are in intermediate exchange (broad signals) as a result of mutual steric interaction in the structure [13]. The flipping rate of Y7 was used as a mobility probe for the comparison of several single-residue mutants of ferrocytochrome c_{553} [26]. In the oxidized c_{553}, four signals are observed for Y7 at 23°C (instead of two in the reduced state). The ring protons of Y44 have not been detected in the oxidized protein at any temperature and this indicates that they are even broader than in the reduced state. The steric hindrance of Y44 in the hydrophobic heme pocket as well as strong paramagnetic shifts (see the unusual shifts of Y44 NH, CαH and $C\beta H_2$ in Table 1) could explain this disappearance. Despite their peculiar chemical shift value, all non-ring protons of the fifth heme ligand H14 have been identified. The two cysteine residues are the two covalent ligands of the heme iron but were easily found. For serines, aspartic acids and asparagine, the AMX systems were always identified, in the same manner as the unique spin systems: 10 glycines, 12 alanines, 5 leucines, 1 isoleucine, 2 valines and 1 threonine were assigned.

3.2. Secondary structure in ferricytochrome c_{553}

Fig. 2 summarizes the sequential and medium-range nOes deduced from the spin system assignment. Nearly all $C\alpha H_{(i)} \rightarrow NH_{(i+1)}$ nOes (except for broad NH such as Gly-12, or overlapping signals such as [Leu-37–Tyr-38] or [Thr-58–Asn-59]) were observed: this is not unexpected in view of the high sample concentration and the maximum value that a $C\alpha H_{(i)}$-$NH_{(i+1)}$ distance can reach (3.5 Å).

Five helical segments, characterized by strong $NH_{(i)} \rightarrow NH_{(i+1)}$ and $C\alpha H_{(i)} \rightarrow NH_{(i+3)}$ nOes, were found: 3→11, 13→18, 33→47, 52→59, 66→79. These results indicate that the secondary structures are highly conserved in the two oxidoreduction states of the cytochrome c_{553}. In the ^{1}H-NMR spectra of the reduced cytochrome, C13 and H14 amide protons were found superimposed and A16 was drastically broadened. The resonance shifts in the ferricytochrome confirm the presence of a helical structure for the segment 13→18. In the NOESY spectrum of the aromatic region, several inter-residue nOes are observed allowing an analysis of the hydrophobic core in the ferricytochrome c_{553}. $H_{2,6}$ protons of Y7 show connectivities to the ring protons of Y75 and L72 protons, while A4 protons exhibit cross-peaks with Y75 ring protons: the N- and C-terminal helices consequently stay in close proximity. Two other tyrosine residues are involved in a crowded nOe network: the side chain of Y38 is close to the C-terminal helix – its $H_{3,5}$ exhibits connectivities with D66, L69 and K70 and $H_{2,6}$ to A73 – and the aromatic ring of Y64 is buried between the adjacent C-terminal helix

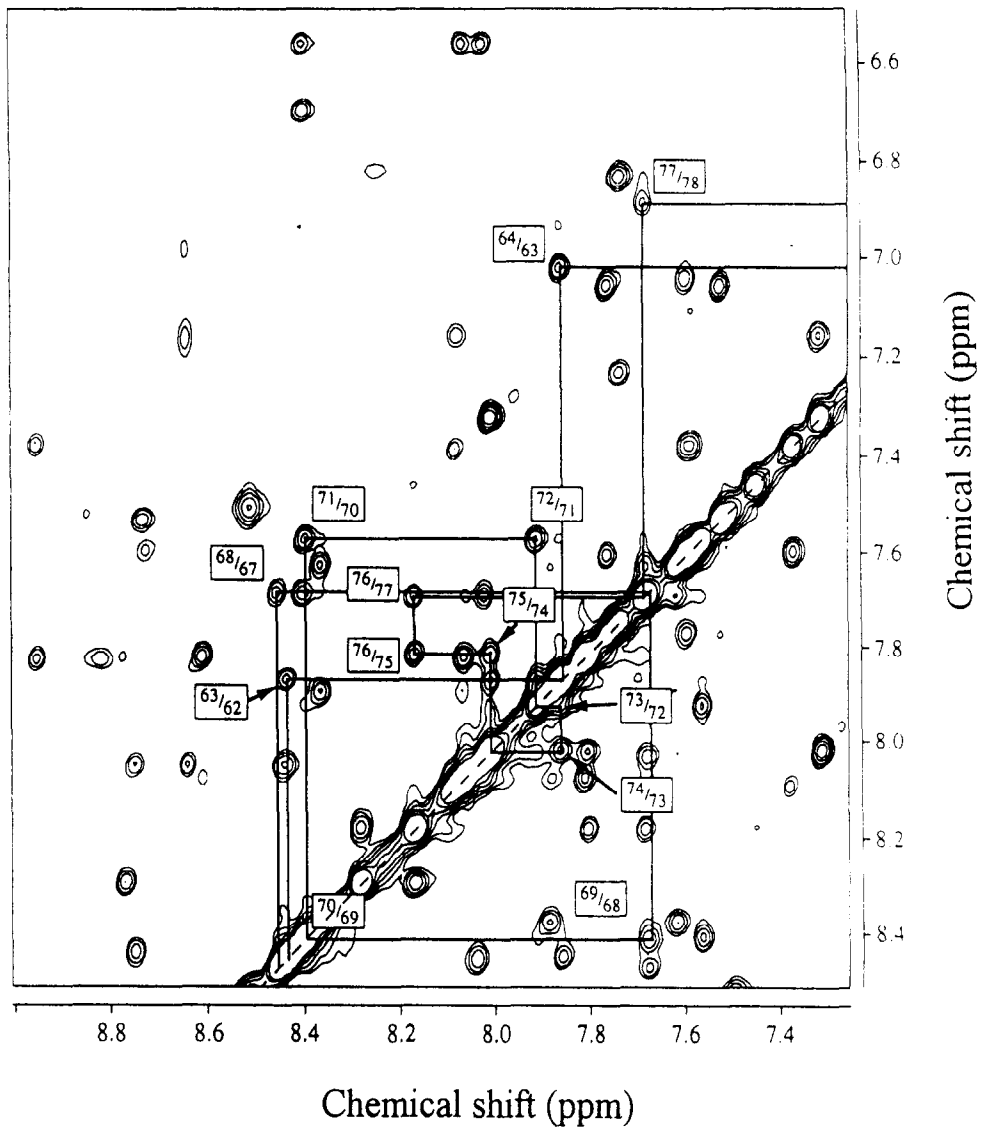

Fig. 1. Expanded region of the 150 ms NOESY spectrum of *D. vulgaris* Hildenborough ferricytochrome c_{553} recorded in H_2O. The $NH_{(i)} \rightarrow NH_{(i+1)}$ cross-peaks corresponding to the C-terminal helix, which is conserved among many cytochromes, are labelled.

(contacts with L69 and L72), the N-terminal helix (contact with L6), the Val-61 and the heme methyl in 2 and methine in 3.

3.3 Chirality of the axial methionine

As the lone pairs on the Met sulfur cannot be seen by NMR, determination of the methionine chirality involves a complete conformational study of the Met side chain. 1D nOe experiments (data not shown) indicate intensive transfer on methyls 2 and 3 and meso-proton in position 20 when the methionine 57 ε-methyl group is irradiated. The reverse experiment (irradiation of the heme methyls and observation of the Met ε-CH3) is unfortunately not feasible due to the respective relaxation rates of these partners (an estimate of the longitudinal self-relaxation rate can be derived from the linewidth, $\Delta\nu_{1/2}$ 30 Hz for heme CH_3 and 100 Hz for Met ε-CH_3). On the basis of these nOes between Met-57 and the heme, one can conclude that the orientation of Met-57 ε-CH_3 is unchanged as compared to the structure obtained by restrained molecular dynamics for the reduced form [13].

As originally proposed by Feng et al. [27], the dipolar contribution to the paramagnetic shifts can be computed using the atomic coordinates of either state [28,29]. The chemical shifts of the amide proton were computed while optimising both the orientation and magnitude of the dipolar field tensor. The convergence of this optimisation is greatly improved by removing the NH of the heme ligands, which are too close to the Fe^{3+} and may thus be affected by the spatial distribution of the unpaired electron. As two families of conformations were found compatible with the NMR data of the reduced state [13], the computation of paramagnetic shifts was carried out on both families. A satisfactory agreement was found between the computed values and the experimental shifts for both families (more than 90% of the residues fits better than 0.1 ppm). These results suggest the lack of major conformational changes associated with oxidoreduction state transitions. Any sizeable shift of the anchoring point of Met-57 side chain (i.e. its Cα) with respect to the heme can thus be ruled out. As three conformational reference points remain nearly unchanged in both oxidation states (the Cα, the

Table 1
Proton chemical shifts (ppm) of ferricytochrome c_{553} at 23°C

	NH (ppm) ox. (red.)	CαH (ppm)	CβH (ppm)	Others (ppm)
Ala(1)				
Asp(2)				
Gly(3)	8.75 (9.02)	3.38; 2.97		
Ala(4)	7.54 (7.78)	2.25	1.10	
Ala(5)	7.06 (7.25)	3.86	1.27	
Leu(6)	7.79 (8.15)	3.78	1.33	(γ) 1.65; (δδ′) 0.44; 0.69
Tyr(7)	7.62 (8.16)	3.59	2.45; 2.31	ring 6.03; 7.00; 7.16
Lys(8)	7.05 (7.41)	3.83	1.81	(γ/δ) 1.49; 1.66; (ε) 2.95
Ser(9)	7.24 (7.87)	4.26	3.81; 3.64	
Cys(10)	7.76 (8.51)	3.45	1.20[a]	
Ile(11)	6.83 (6.81)	3.70	1.80	(γ) 1.17; 1.12
Gly(12)				
Cys(13)	7.86 (6.44)	5.66	3.57	
His(14)	10.46 (6.45)	9.26	15.52; 6.95	πNH 14.90
Gly(15)	9.92 (7.74)	5.51; 4.72		
Ala(16)	8.76 (9.47)	4.84		
Asp(17)	8.44 (7.82)	4.93	3.40; 2.82	
Gly(18)	8.03 (7.06)	5.02; 4.37		
Ser(19)	8.63 (7.70)	4.60	2.75; 2.42	
Lys(20)	8.44 (6.81)	4.77	1.97; 1.86	(γ/δ) 2.05; 2.60; (ε) 3.33
Ala(21)	9.45 (8.48)	5.01	1.40	
Ala(22)	8.69 (7.30)	4.13	−0.53	
Met(23)	8.57 (9.20)	3.58	1.45; 0.77	(γ) 1.21; 1.38
Gly(24)	8.09 (8.42)	3.96; 3.51		
Ser(25)	7.17 (7.91)	4.29	3.31; 3.13	
Ala(26)	7.39 (7.85)	3.83	0.27	
Lys(27)	8.02 (8.38)	4.58	1.65	(γ/δ) 1.54; 1.79; (ε) 2.94
Pro(28)	5.76	3.06; 2.49		(γ) 2.19; (δ) 4.23; 3.87
Val(29)	9.56 (7.52)	4.48	2.41	(γ) 1.50; 1.87
Lys(30)	8.08 (7.23)	4.25	1.70; 1.52	(γ/δ) 1.30; 2.17
Gly(31)	9.81 (9.59)	4.25; 3.77		
Gln(32)	7.52 (7.57)	4.38	2.02; 1.80	(γ) 2.19; 2.46 (δNH_2) 7.51; 8.53
Gly(33)	8.85 (8.97)	4.10; 3.87		
Ala(34)	8.79 (8.96)	3.66	1.27	
Glu(35)	8.61 (8.82)	3.89	1.97; 1.91	(γ) 2.21
Glu(36)	7.79 (7.96)	3.91	1.91; 2.04	(γ) 2.41; 2.21
Leu(37)	8.08 (8.47)	3.40	1.55; 1.67	(δδ′) 0.47; 0.35
Tyr(38)	8.08 (8.51)	3.47	2.86; 2.63	ring $H_{2,6}$ 6.58 $H_{3,5}$ 6.71
Lys(39)	8.05 (8.22)	3.43	1.65; 1.77	(γ/δ) 1.56; 1.27; (ε) 2.85
Lys(40)	7.69 (7.96)	3.06	1.37; 1.78	(γ/δ) 1.21; 1.09
Met(41)	7.63 (8.23)	4.17	1.88; 2.93	(γ) 0.32
Lys(42)	8.38 (8.42)	3.84	1.38; 1.54	(γ/δ) 0.87; (ε) 2.74; 2.94
Gly(43)	7.90 (7.66)	4.34; 3.60		
Tyr(44)	9.24 (8.52)	5.52	4.79; 4.41	
Ala(45)	8.76 (8.02)	4.62	1.88	
Asp(46)	8.29 (7.76)	4.96	3.19; 2.79	
Gly(47)	8.17 (7.58)	4.54; 4.20		
Ser(48)	9.25 (8.85)	4.53	4.12; 3.85	
Tyr(49)	7.46 (7.03)	4.50	2.99; 2.20	ring $H_{2,6}$ 6.43 $H_{3,5}$ 6.83
Gly(50)	6.64 (6.50)	4.73; 3.03		
Gly(51)	9.95 (10.41)	4.34; 3.51		
Glu(52)	8.74 (9.08)	3.93	1.82	(γγ′) 2.09
Arg(53)	7.61 (8.24)	4.43	1.23; 0.96	(γ/δ) 2.08; 0.57
Lys(54)	7.39 (7.42)	4.43	2.18; 2.10	(γ/δ) 1.90; 1.75; (ε) 2.68
Ala(55)	8.96 (8.49)	4.72	1.65	
Met(56)	7.82 (7.29)	4.55	1.44	
Met(57)	11.31 (5.76)	8.82		(ε) −10.3
Thr(58)	9.03 (8.33)	5.03	5.19	(γ) 2.01
Asn(59)	9.03 (6.93)	5.00	3.24; 3.19	
Ala(60)	9.38 (6.41)	4.82	3.50	
Val(61)	9.18 (6.72)	5.15	2.92	(γ) 2.19; 1.04
Lys(62)	8.44 (7.42)	4.46	2.48; 2.39	(δ) 2.01; 1.93; (γ) 1.70 (ε) 3.26

For comparison the NH shifts of the reduced cytochrome under the same conditions have been included.
[a]Observed at 37°C.

Table 1 (*continued*)

	NH (ppm) ox. (red.)	CαH (ppm)	CβH (ppm)	Others (ppm)
Lys(63)	7.85 (7.44)	4.26	1.61; 1.54	(γ/δ) 0.92; 0.67; (ε) 2.82
Tyr(64)	7.02 (6.92)	4.83	3.17; 2.58	ring $H_{2,6}$ 6.96 $H_{3,5}$ 6.44
Ser(65)	9.70 (9.84)	4.59	4.40; 4.04	
Asp(66)	9.09 (9.14)	4.41	2.70	
Glu(67)	8.46 (8.57)	3.80	2.02; 1.82	(γ) 2.23; 2.10
Glu(68)	7.69 (7.89)	3.40	2.55	(γ) 2.27; 2.01
Leu(69)	8.42 (8.70)	3.51	2.26; 1.83	(γ) 0.97; (δδ′) 0.75; 0.59
Lys(70)	8.41 (8.72)	3.48	1.55	(γ/δ) 1.13; 0.65 (ε) 2.41; 2.25
Ala(71)	7.58 (7.92)	4.01	1.13	
Leu(72)	7.93 (8.56)	3.33	1.34; 0.82	(γ) 0.03; (δδ′) −0.02; −0.62
Ala(73)	7.88 (8.65)	3.23	1.28	
Asp(74)	8.03 (8.40)	3.96	2.51	
Tyr(75)	7.82 (8.20)	3.76	2.85; 2.43	ring 6.41
Met(76)	8.18 (8.91)	3.28	1.75 1.28	(γγ′) 0.14; 1.52
Ser(77)	7.69 (8.00)	4.28	4.07; 3.73	
Lys(78)	6.89 (7.04)	4.27	1.89 1.52	(γ) 1.37; (δ) 1.23
Leu(79)	6.84 (6.86)	3.73	1.60	(γ or β′) 1.36; 1.32 (δδ′) 0.49; 0.36

For comparison the NH shifts of the reduced cytochrome under the same conditions have been included.
[a]Observed at 37°C.

εCH_3 and the Fe-S bond), one can thus safely conclude that the Met-57 side-chain has the same conformation and chirality in both states.

3.4. *Heterogeneity in ferricytochrome c_{553} chemical shifts*

H-NMR spectra (NOESY) of oxidized cytochrome c_{553} show a duplication of numerous cross-peaks corresponding to heme group protons and polypeptide chain protons. The intensity ratio between major and minor cross-peaks is around 10 1. The most affected resonances turn out to be either in the N-terminal or the central helices as well as a few scattered residues (S65, D66, A71, D74, S77). These last three NH are on the solvent-accessible side of the C-terminal helix. A third set of peaks was even found for D46, G47, and S48. The induced chemical shift differences between the major and minor species are smaller than ±0.1 ppm. The presence of the same ratio of both conformations is observable over a long period of time and under various experimental conditions (time, temperature, salt concentration, and pH in either native or recombinant protein). Mass spectrometry provides evidence of a +16 and +32 mass increase which could be associated with oxidative damage of a methionine (sulfoxide and sulfone derivatives). One cannot rule out the possibility that this is related to the low oxidoreduction potential of cytochrome c_{553}. The high excess of sodium dithionite necessary to reduce this low oxidoreduction potential cytochrome acts probably in the reduction of the methionine side chain; Senn et al. [10] observed a second conformation of reduced cytochrome c_{553} which disappeared after a few hours of incubation of the reduced protein in an anaerobic atmosphere.

4. Discussion

The complete proton assignment of oxidized and reduced cytochrome c_{553} from *D. vulgaris* Hildenborough has been achieved using 1D- and 2D-NMR. The sequential connectivities demonstrate that the protein secondary structure is well conserved from one oxidation state to the other. Five helices are involved in the heme binding and environment. Three (N-terminal, C-terminal and central helices) are conserved structural elements in all *c*-type cytochromes and a fourth, near the sixth heme ligand (M57), is a specific feature of cytochrome c_{553}.

The following observations indicate that the structure of the molecule in the oxidized form is more compact than in the reduced form: (i) an increased number of NH remain unexchanged in D_2O samples in the oxidized form (note that a reduced sample is always prepared from an oxidized one); (ii) larger amounts of medium-range nOes ($C\alpha H_{(i)} \rightarrow NH_{(i+1)}$, $C\alpha H_{(i)} \rightarrow NH_{(i+3)}$, $C\alpha H_{(i)} \rightarrow NH_{(i+4)}$ are observed, despite the notable line broadening observed in the oxidized form spectra which would not favour the observation of such medium range nOes: stronger nOe provides indirect evidence of a longer effective correlation time, i.e. reduced internal flexibility; (iii) qualitative interpretation of the flipping rates of the various tyrosines in both oxidoreduction states supports the idea of increased steric hindrance but further studies of the temperature dependence of ring proton coalescence will be necessary before a final conclusion can be drawn. This result is different from the reported properties of mitochondrial and bacterial cytochromes for which it is generally thought that the reduced form is less flexible than the oxidized form. One of the main differences of *Desulfovibrio* cytochrome c_{553} (versus other *c*-type cytochromes) resides in its oxidoreduction potential which is 300 mV lower than for mitochondrial cytochromes. The fact that the most stable state is the reduced form for an aerobic organism and the oxidized one for anaerobic bacteria is not unexpected and is probably correlated with the different H-bond network in these molecules [13–15].

As the paramagnetic shifts can be fairly well computed using the coordinates of the reduced form, one can safely conclude that no major conformational changes occur between both forms. However, the slight discrepancies detected between the computed and observed paramagnetic shifts suggest minor structural adjustment of the secondary structures, one with respect to the other. Long-range nOes demonstrate a

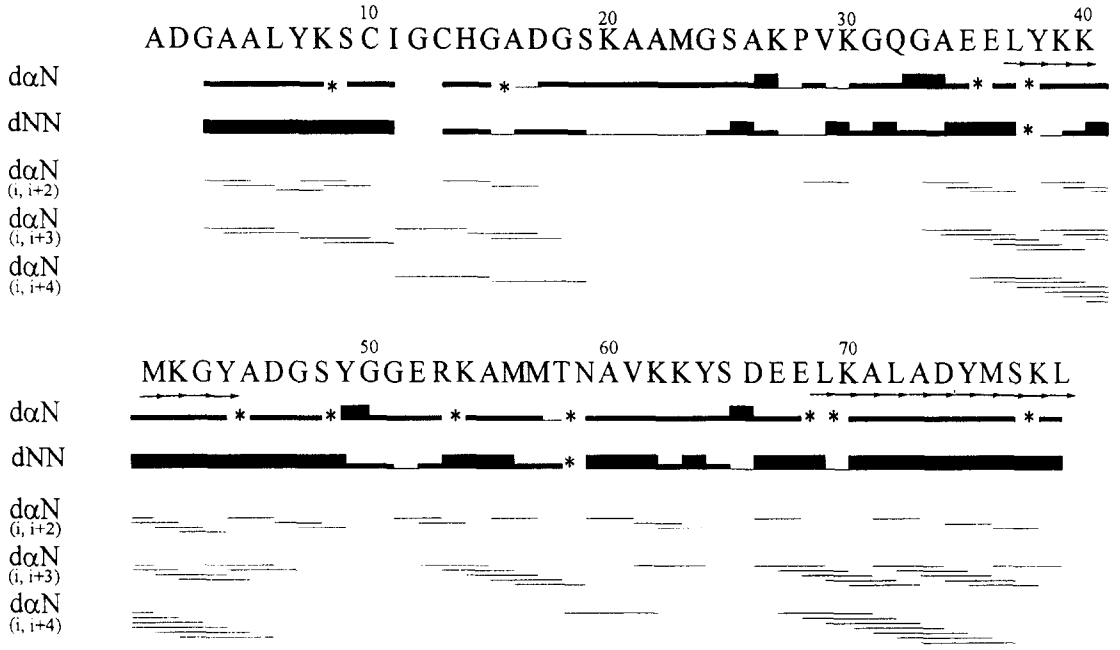

Fig. 2. Summary of the sequential connectivities which support the resonances assignment in the ferricytochrome c_{553} from *D. vulgaris* Hildenborough. Sequential nOes which are not observable due to spectral overlap are indicated by asterisks. The nOe intensities are indicated by the black bars. Arrows indicate residues 37–44 and 69–79 with slowly exchanging protons (lifetime greater than a few weeks at room temperature and pH 5.9).

modification of the L72 and L69 side chain orientation. These changes are correlated to packing modification of the C-terminal and central helices which would provide more compact folding of the molecule. The other modifications inferred from chemical shift variations affect the neighbourhood of M23 and K54 on the top of the heme crevice. The structural variations due to the change of oxidation state are currently being studied in our laboratories in terms of long-range constraints. In contrast to a previous work on this cytochrome which suggested a significant modification of the axial ligand chirality [10], our results are more in agreement with small structural variations as reported for other cytochromes *c* from X-ray structures [30–32]. The preliminary analysis of long range nOes suggests a change in the hydrogen bonding network around the heme, which may directly result from the +1 charge difference between the two oxidoreduction states.

Berghuis and Brayer [16] have demonstrated subtle conformational changes associated with oxidoreduction transitions. Oxidation state-dependent changes are expressed for the most part in terms of adjustments to heme structure, movement of internally bound water molecules rather than polypeptide chain shifts which are found to be minimal. The water molecule (Wat166) is a major factor in stabilizing both oxidation states of the mitochondrial cytochrome. Y67, T78 and N52 are hydrogen bonded to this internal water molecule. From a sequence alignment on the basis of the structure of horse cytochrome *c* and *D. vulgaris* Hildenborough cytochrome c_{553} that we previously proposed [12], one can observe that the corresponding segments to residues 37–59 (horse cytochrome *c* numbering) are missing in cytochrome c_{553}; the 81–85 segment is a structurally different region in cytochrome c_{553} as it is the end of the 6th axial ligand containing helix. From their computation of paramagnetic chemical shifts, Turner and Willams [29] have reported some redox-related movement in the vicinity of Trp-59 in horse cytochrome *c*, which is a segment missing in cytochrome c_{553}. The improvement of structural data on both oxidation states of *D. vulgaris* Hildenborough cytochrome c_{553}, and the identification of structural water molecules will lead to a better understanding of the oxidoreduction modulation of cytochrome c_{553}. Qi et al. [33] have used NMR spectroscopy to demonstrate structural water molecules in oxidized and reduced horse heart cytochrome *c*. In our case, the identification of the structural water molecules is made difficult by the presence of several hydroxyl groups in the putative sites and the lack of X-ray structure. Site directed mutagenesis is also currently being used to identify the key residues involved in oxidation state stabilisation.

References

[1] Moore, G.R. and Pettigrew, G.W. (1990) Cytochromes *c*. Evolutionary, Structural and Physicochemical Aspects, Springer, Berlin.
[2] Koshy, T.I., Luntz, T.L., Schejter, A. and Margoliash, E. (1990) Proc. Natl. Acad. Sci. USA 87, 8697–8707.
[3] Luntz, T.L, Schejter, A., Garber, E.A.E. and Margoliash, E. (1989) Proc. Natl. Acad. Sci. USA 86, 3524–3528.
[4] Caffrey, M., Davidson, E., Cusanovich, M. and Daldal, F. (1992) Arch. Biochem. Biophys. 292, 419–426.
[5] Mauk, A.G. (1991) Structures and Bonding 75, Springer, Berlin.
[6] Mus-Veteau, I., Dolla A., Guerlesquin, F., Payan, F., Czjzek, M., Haser, R., Bianco, P., Haladjian, J., Rapp-Giles, B., Wall, J.D., Voordouw, G. and Bruschi, M. (1992) J. Biol Chem. 267, 16851–16858.
[7] Korszun, Z.R and Salemme, F.R. (1977) Proc. Natl. Acad. Sci. USA 74, 5244–5247.
[8] Morelle, N., Simorre, J.-P., Caffrey, M., Meyer, T., Cusanovich, M. and Marion, D. (1995) FEBS Lett. 365, 172–178
[9] Bersch, B., Brutscher, B., Meyer, T.E. and Marion, D. (1995) Eur. J. Biochem. 227, 249–260.
[10] Senn, H., Guerlesquin, F., Bruschi, M. and Wüthrich, K. (1983) Biochim. Biophys. Acta 748, 194–204.

[11] Nakagawa, A., Higuchi, Y., Yasuoka, N., Katsube, Y. and Yagi, T. (1990) J. Biochem. 108, 701–703.
[12] Marion, D. and Guerlesquin, F. (1992) Biochemistry 31, 8171–8179.
[13] Blackledge, M.J., Medvedeva, S., Poncin, M., Guerlesquin, F., Bruschi, M. and Marion, D. (1995) J. Mol. Biol. 245, 661–681.
[14] Blackledge, M.J., Guerlesquin, F. and Marion, D. (1995) Nat. Struct. Biol. 2, 532–535.
[15] Blackledge, M.J., Guerlesquin, F. and Marion, D. (1996) Proteins: Struct. Funct. Genet. 24, 178–194.
[16] Berghuis, A.M and Brayer, G.D (1992) J. Mol. Biol. 223, 959–976.
[17] Blanchard, L., Marion, D., Pollock, B., Voordouw, G., Wall, J., Bruschi, M. and Guerlesquin, F. (1993) Eur. J. Biochem. 218, 293–301.
[18] Wagner, G. and Wüthrich, K. (1979) J. Magn. Reson. 33, 675–680.
[19] Unger, S.W., Lecomte, J.T.L. and La Mar, G.N. (1985) J. Magn. Reson. 64, 521–526
[20] Banci, L., Bertini, I., Luchinat, C., Piccioli, M., Scozzafava, A. and Turano, P. (1989) J. Inorg. Chem. 28, 4650–4656.
[21] States, D.J., Haberkorn, R.A and Ruben, D.J. (1982) J. Magn. Reson.48, 286–292.
[22] Rance, M., Sørensen, O.W., Bodenhausen, G., Wagner, G., Ernst, R.R. and Wüthrich, K. (1983) Biochem. Biophys. Res. Commun. 117, 479–485.
[23] Davis, D.G. and Bax, A. (1985) J. Am. Chem. Soc. 107, 2820–2821.
[24] Macura, S., Huang, Y., Suter, D. and Ernst, R.R (1981) J. Magn. Reson. 43, 259–281.
[25] Plateau, P. and Guéron, M. (1992) J. Am. Chem. Soc. 104, 7310–7311.
[26] Blanchard, L., Dolla, A., Bersch, B., Forest, E., Bianco, P., Wall, J., Marion, D. and Guerlesquin, F. (1994) Eur. J. Biochem. 226, 423–432.
[27] Feng, Y., Roder, H. and Englander, S.W. (1990) Biochemistry 29, 3494–3504.
[28] Timkovich, R. and Cai, M. (1993) Biochemistry 32, 11516–11523.
[29] Turner, D.L. and Williams, R.J.P. (1993) Eur. J. Biochem. 211, 555–562
[30] Matsuura, Y., Takano, T. and Dickerson, R.E. (1982) J. Mol. Biol. 156, 389–409.
[31] Takano, T. and Dickerson, R.E. (1981) J. Mol Biol. 153,79–94.
[32] Takano, T. and Dickerson, R.E. (1981) J. Mol. Biol. 153, 95–115.
[33] Qi, P.X., Urbauer, J.L., Fuentes, E.J., Leopold, M.F. and Wand, A.J. (1994) Nat. Struct. Biol. 1, 378–381.